



## OPEN Development of a global thermal detection index to prioritize primate research with thermal drones

Eva Gazagne<sup>1✉</sup>, Russell J. Gray<sup>2</sup>, Serge Wich<sup>3</sup>, Alain Hambuckers<sup>1</sup> & Fany Brotcorne<sup>1</sup>

Thermal Infrared (TIR) drones are emerging as effective tools for wildlife ecology monitoring and are increasingly employed in primate surveys. However, systematic methods for assessing primate detectability are lacking. We present a comprehensive approach utilizing a novel Thermal Detection Index (TDI) to evaluate the potential of TIR drones for primate monitoring. We developed TDIs for 389 primate species, considering activity patterns, locomotion types, body mass, densities, habitat utilization, and sleeping behaviors during diurnal and nocturnal surveys. Through the integration of TDIs with primates' distribution and climatic variables (average annual temperature, precipitation, and wind speed), we established a Global TDI Suitability Score aimed at pinpointing species and regions most compatible with TIR drone-based monitoring. Atelidae, Cercopithecidae, and Indridae showed the highest TDI values, suggesting their suitability for TIR-drone surveys. We identified optimal regions in Africa, Asia and Latin America for primate monitoring with TIR drones, driven by favorable ecological conditions, habitat types, and high TDI species diversity. However, local ecological factors and regulatory frameworks also influence drone survey feasibility, necessitating careful consideration prior to implementation. Overall, our study provides a valuable framework for prioritizing primate species and regions for TIR drone-based monitoring, facilitating targeted conservation efforts and advancing primate monitoring research.

Drones have recently emerged as tools in wildlife ecology, facilitating studies in population estimates and behavioral ecology, while providing remote-sensing data at fine spatial and temporal scales<sup>1–4</sup>. The integration of thermal infrared (TIR) imaging and drone technology (hereafter TIR drones) in ecological studies holds great promise for effective species monitoring in conservation efforts<sup>5</sup>. TIR drones facilitate the detection of animals based of their body heat, allowing wildlife censuses and identification of species not visible to the naked eye or through red, green, blue (RGB) imagery (e.g., the detection of cryptic species or conducting nocturnal surveys)<sup>4</sup>.

The potential to detect and enumerate primate populations through TIR drone technology presents a promising avenue for resource and labor-efficient, non-invasive, long-term monitoring programs<sup>6–9</sup>. However, the effectiveness of employing thermal drones for primate monitoring varies across species, landscape and habitat types, influenced by various ecological traits and factors that affect the detection probability via TIR imagery. Activity patterns play a crucial role; nocturnal species might be challenging to detect during diurnal surveys as they could sleep in tree holes, while diurnal species might be difficult to detect during nocturnal surveys if they sleep in caves<sup>5,10</sup>. Locomotion patterns also contribute; with highly arboreal species effectively detected and counted in forested areas, and ground-dwelling species efficiently monitored in open terrain but remaining undetected under the tree canopy<sup>10–14</sup>. Ecological factors inherently linked to the level of arboreality or terrestriality of species, such as vegetation type, canopy density, canopy height, and terrain elevation, influence detection probabilities in TIR images<sup>5,15,16</sup>. Animal body size and group size also impact detection, with smaller species living solitary or in small groups more likely to be missed in aerial surveys<sup>7,17</sup>. Generally, TIR drone surveys are more suitable for surveying large-bodied species occurring in high densities or ranging over small areas<sup>11,12</sup>. Finally, behavioral responses to the drone, such as animals becoming startled or fleeing, compromise reliable detection and counting<sup>5,6,12,13</sup>. These ecological traits and behaviors necessitate a thorough assessment to determine which primate species can potentially be effectively monitored using TIR drones. Moreover, the widespread implementation of drones to study primate population habitat, abundance, and behavior, faces

<sup>1</sup>Unit of Research SPHERES, University of Liège, Quai van Beneden, 22, Liège 4020, Belgium. <sup>2</sup>Save Vietnam's Wildlife, Cuc Phuong National Park, Nho Quan, Ninh Binh Province, Vietnam. <sup>3</sup>School of Biological and Environmental Sciences, Liverpool John Moores University, Liverpool, UK. ✉email: evagazagne@live.fr

limitations, such as flight range, regulatory frameworks (e.g., legislation and challenges and expenses to obtain permits), data-processing time, and the lack of methodological validation<sup>1,3,18</sup>. Therefore, researchers need preliminary knowledge to justify investing funds and effort in developing research projects incorporating this technology as an alternative to traditional survey techniques.

This paper aims to leverage existing primate species data to construct a Thermal Detection Index (TDI) that will assess species, genera, and families most amenable to monitoring via thermal drones. Survey methods such as flight height, flight speed and pattern, as well as gimbal angle, can impact TIR drone detection probabilities, influencing both detection resolution and animal response to the drone<sup>5,11,19–21</sup>. To simplify TDI implementation, we presume that each flight parameter is ‘optimal’ for each species following recommendations outlined in Burke et al. (2018)<sup>22</sup> to maximize detection, providing the minimum resolution for animals to be visible and identified (e.g., according to drone TIR sensor pixel resolution, lens characteristics, and target species body size<sup>11</sup>) while minimizing disturbance<sup>7,13,23,24</sup>. Finally, TIR drone detections will also depend on the time of the survey, with nocturnal surveys more effective when there are larger temperature differences between targeted species and their surroundings<sup>13,21,25</sup>. While nocturnal detections generally yield higher success rates due to greater thermal contrast, it is essential to assess both nocturnal and diurnal scenarios to account for species’ activity patterns, resting sites, and for situations where nocturnal surveys are not feasible. Therefore, we aim to develop nocturnal and diurnal TDI values for various primate species (representing 78 genera) that will integrate species’ activity pattern, locomotion type, body mass, densities, habitat use, and sleeping behavior.

Beyond nocturnal and diurnal TDIs for primate species, TIR drone surveys are often constrained by weather conditions (e.g., ambient temperature, precipitation, wind speed, etc.). These weather-related factors not only impact the image quality and animal detection but also narrow the window of opportunity for aerial surveys or deploying drones on-demand<sup>22,26–29</sup>. To address these limitations and evaluate the reliability of TIR drone surveys, we aimed to develop a Global TDI Suitability Score, which integrates geospatial components to examine the relationship between primate species distribution, TDIs, and climatic variables that affect drone flights. Ultimately, our study aimed to identify areas more suitable for sustained TIR drone-based monitoring of primates by establishing methodological tools that enable researchers to find TDIs for their study species and assess the reliability of TIR drone use given climate, habitats, and ecological traits.

## Methods

### Data acquisition and processing

To construct a Thermal Detection Index (TDI), we extracted comprehensive information from the IUCN RedList of Threatened Species database (2024)<sup>30</sup>, encompassing species taxonomy (Family, Genus, Common Name, Scientific Name), along with conservation status, and habitat preferences across various ecosystems (e.g., Forest, Savannah, Shrubland, Grassland, Wetland, Rocky area, Desert, Artificial). We completed this dataset with some important ecological traits of the world’s primates, including diel activity (i.e. Nocturnal, Diurnal, Cathemeral), locomotion type (i.e. Arboreal, Terrestrial, Semi-terrestrial), body mass (kg), average home range size (km<sup>2</sup>), and mean number of individuals per group extracted from Galán-Acedo et al. (2019)<sup>31</sup> database ( $N = 389$  species). We assessed species mean population density based on mean number of individuals per group and average home range size (individuals per sq km). Additionally, we incorporated information on sleeping habits, considering nesting behaviors, caves, cavities, and tree hole usage by species<sup>32</sup>. The finalized database used for thermal detection index construction is available in Supplementary Material 1. To produce a Global TDI Suitability Score, we integrated TDI estimates from the current study with primate species distribution polygons, average annual temperature (°C), average annual wind speed (m.s<sup>-1</sup>), and annual precipitation (mm) across global regions<sup>33</sup> (Table 1).

### Thermal detection index (TDI) construction

The Thermal Detection Index (TDI) is separately calculated for Nocturnal and Diurnal surveys. It is derived as the cumulative score of three equally weighted traits, the Habitat Average ( $Hab_{av}$ ), Body Mass (BM), and population Density (Dens):

$$TDI = Hab_{av} + BM + Dens$$

Data	Description	Rationales
TDI Estimates	TDI for each species, established in the current paper	We connect this data to the distribution data as a weighted score
IUCN Redlist primate distribution polygons <sup>30</sup>	Distribution polygons of all assessed primate species in the IUCN Redlist of Threatened Species database	The maps provide a spatial area in which the primates occur
Average annual temperature (°C) <sup>33</sup>	Monthly temperatures averaged from 1970–2000, averaged into a single annual raster layer	Thermal imaging of mammals is most effective in colder environments as it enhances thermal contrast by capturing the difference in temperature between the target animal and the colder surroundings <sup>13,21,22,25</sup>
Average annual wind speed (m s <sup>-1</sup> ) <sup>33</sup>	Monthly wind speed averages from 1970–2000, averaged into a single annual raster layer	Strong wind speed affects the ability to operate drones, but also decrease thermal contrast between animals and their background. The maximum wind speed resistance of small common drones is usually 10 m/s <sup>27,28</sup>
Annual precipitation – Bio12 (mm) <sup>33</sup>	Average annual precipitation from 1970–2000	Rainfall and humidity may prevent drone flights and functionality and distort the results of thermographic imaging. Increased frequency of rainfall raises the likelihood of disruptions to flight plans <sup>22,26,28</sup>

**Table 1.** Data source to construct the global thermal detection index (TDI) suitability score across primates’ natural range.

We assume that each trait has an equivalent impact on detectability, with locomotor behavior being independent of body mass<sup>34</sup>.

To consider ecological influences on detectability, a habitat scoring system is designed to assess the likelihood of successful thermal detection across varied environments. It utilizes a five-point scale from 0 to 4, denoting progressively lower to higher probabilities of successful thermal detection (Table 2). In cases where species inhabit multiple habitats, we computed a mean score of these habitats ('Hab<sub>av.</sub>'). To obtain this score, we considered both diurnal and nocturnal detection scenarios (i.e., diurnal versus nocturnal surveys using a TIR drone), as well as primate species' activity patterns and preferred habitats (i.e., the dominant substrate or environment they used). For example, consider species exhibiting diurnal activity patterns, detecting them during nocturnal surveys within sleeping trees is more feasible compared to daytime surveys due to elevated temperatures, increased scattering of groups, or individuals foraging on the ground. However, this does not apply if the species habitually rest in caves. Nocturnal species are more detectable during their active night-time period, as they tend to occupy tree holes and cavities during the day. Therefore, species found sleeping in caves or in cavities/tree holes receive a detection score of zero during diurnal thermal drone surveys. Species locomotion's type served as a potential indicator of vertical forest use (e.g., use of emergent layer, understory, or ground strata), acting as a proxy for vertical TIR detection probability. For example, arboreal species (AR) are more readily detectable in tropical forested habitats compared to terrestrial (T) or semi-terrestrial (ST) species, which are more easily detected in savannah, grassland, and desert environments. Therefore, the detection score accounts for ecological, physiological, behavioral, and temporal variations that may influence primate detectability in a given habitat.

Thereafter, to obtain the factors Body Mass ('BM') and Density ('Dens'), we categorized the data for each primate species into four categories based on the quartile summaries (scored as '1', '2', '3', and '4'). These categories represent relative sizes and population densities that may increase detectability by TIR drone (i.e., larger animals with bigger groups are easier to detect than smaller, solitary animals). Lower scores correspond to species with lower body mass or low population density, implying reduced body surface temperature and more dispersed thermal detection. Conversely, higher scores indicate species with greater body mass and higher population

		Detection score			Rationale
		Noc. Survey	Diu. Survey		
Habitats	Description	AR-T-ST	AR	T-ST	
					Detections during nocturnal surveys are higher as the contrast between external temperature, and consequently the substrate and the detected species is higher
Forest	Tropical wet forest, cloud forest, dry forest, montane forest, temperate forest and semi-deciduous forest	3	2	1	Arboreal species are easier to detect in forested area, and terrestrial or semi-terrestrial species easier to detect in more open habitats during the day. Nocturnal detections remain consistent for species sleeping in trees
Savannah	Dry and moist savannah forest and savannah mosaics	4	2	3	Savannahs offer good vertical visibility for TIR drones to detect primates. The scattered trees and open grasslands facilitate monitoring, especially for more terrestrial species <sup>16,36</sup>
Shrubland	Tropical moist, dry, temperate, and high altitude ecosystems dominated by shrubs (i.e. shrubs, brush and bush)	3	2	2	TIR drones may face challenges in shrublands due to the moderate or low visibility, as well as lower canopy height. Detection of primates in these habitats may be limited in dense shrubby areas or the understory <sup>15,28</sup>
Grassland	Tropical dry and seasonally wet, tropical high altitude, and temperate ecosystems mainly composed of grasses and other herbaceous plants	4	3	3	TIR drones excel in grasslands, providing excellent visibility to detect primates. Monitoring in these open areas allows for efficient observation of primate movement and behavior <sup>16,28</sup>
Wetlands	Swamps, flooded forest, swampy forest, wetlands, mangroves, permanent or seasonal rivers, streams, or creeks	3	2	1	Wetlands present varying visibility, but TIR drones can be valuable for detecting primates in the open areas. Terrestrial species might have low visibility in wetland areas during the day <sup>16,36</sup>
Rocky Areas	Inland cliffs and mountain peaks	4	3	3	TIR drone surveys may face navigational challenges in rocky areas, but this habitat offers good visibility to detect primates in not too hot conditions
Desert	Temperate ecosystems	4	0*	2	TIR drones may have good visibility in deserts, enabling the detection of primates. Some terrestrial species might be visible in desert habitats during the day <sup>16</sup> (*no arboreal species occur in desert)
Artificial	Heavily degraded former forest, plantations, pastureland, arable lands, rural gardens, and urban areas	4	3	2	Artificial habitats typically feature more open landscapes than forested habitats and are often situated in flat terrain, enhancing primate detection. Additionally, urban or artificial settings might attract species, offering some visibility during the day, but visibility of terrestrial species will be reduced <sup>20,25,35</sup>

**Table 2.** The habitat scoring system (cf. Hab<sub>av.</sub>) is classified into a five-point scale for primate species across different habitats for both Nocturnal (Noc.) and Diurnal (Diu.) Drone surveys using thermal infrared imagery. The habitat description includes all ecosystems in which primates occur. Scores assess the detectability of primate species during different survey types based on habitat characteristics and species locomotion type: arboreal (AR), terrestrial (T), semi-terrestrial (ST). Note. Nocturnal and cathemeral species were exclusively arboreal, while terrestrial and semi-terrestrial species were solely diurnal. If species are found sleeping in caves, cavities, or tree holes, then detection in all habitats during thermal drone surveys will be null, resulting in Hab<sub>av.</sub> = 0.

density, suggesting an elevated likelihood of detection using thermal imagery via drone surveys. The dataset and R script employed to compute TDI are available in supplementary (Supplementary Material 2).

### Global TDI suitability score

To generate a global Thermal Detection Index (TDI) layer, we employed a geospatial processing approach. First, we imported a multi-polygon shapefile containing all assessed primate distribution ranges from the IUCN Red List of Threatened Species using the *sf* package<sup>37</sup>. We then omitted the species for which we were not able to assess the TDI ( $N=132$  species). Next, we fused the subspecies data within the distribution shapefiles to the species level. Finally, we joined the TDI values with the shapefile object based on shared species name.

Subsequently, we used the *raster* package<sup>38</sup> and implemented a loop function to rasterize individual species distribution polygons. This function assigned all cell values within each species' distribution with its associated TDI values. The function iterated through each individual species' range polygon, accumulating TDI values, averaging TDI values, and calculating standard deviations in overlapping cells (Fig. 2. a.) and then adding them to a collective raster at 0.5 arcmin resolution. The cumulative TDI tends to exaggerate the impact of species with extreme TDI values, leading to scores that may align more with species richness than thermal detection (Fig. 2. b.). In contrast, averaging the values in each grid cell prevents species with extremely high or low TDI values from disproportionately influencing the overall Suitability score, while the standard deviation reflects variability in species' TDI values in a given grid cell. We conducted this process separately for both Nocturnal and Diurnal scenarios. Consequently, we obtained individual raster layers representing the TDI values of all species ( $N=389$ ) for both Nocturnal and Diurnal surveys. Afterward, we computed the mean values derived from both Nocturnal and Diurnal TDI layers to generate an average TDI raster layer (cf. steps 1 to 4 in the R script provided in SupplementaryMaterial 3).

The average TDI layer ('TDIav') was then weighted by average annual temperature ('Temp'), wind speed ('Wind'), and precipitation ('Prec') raster layers. As a first step, the input rasters were rescaled and standardized at a 0–1 scale. Subsequently, we assigned weights to each variable to denote their influence on the overall suitability score<sup>39</sup>. Specifically, average TDI received a weight of 1, while temperature, wind speed, and precipitation were assigned weights of -1, indicating an inverse relationship (i.e. higher values of environmental variables contributes to a lower average TDI score). Thereafter, the combined suitability score was computed as the weighted average of the rescaled variables<sup>40</sup>. This process involved summing the products of each rescaled variable and its corresponding weight, and then dividing this sum by the total sum of weights. Finally, to obtain the final TDI Suitability Score for each grid cell, we subtracted the combined score from 1 (cf. steps 5 to 7 in the R script provided in Supplementary Material 3):

$$TDI \text{ Suitability Score} = 1 - \frac{(\text{scaled TDIav} \times \text{wTDIav} + \text{scaled Temp} \times \text{wTemp} + \text{scaled wind} \times \text{wWind} + \text{scaled Prec} \times \text{wPrec})}{(\text{wTDIav} + \text{wTemp} + \text{wWind} + \text{wPrec})}$$

The resulting TDI Suitability Score represents the overall suitability of each grid cell for TIR drone monitoring of primates, taking into account both species-specific TDI values and environmental factors.

To refine the final TDI Suitability Score raster, we exclusively retained suitability scores in the last quartile ( $\geq 0.75$ ), indicating areas with high suitability. We constructed a polygon from the resulting raster layer and intersected it with: (1) a world map to determine the countries associated with the highest suitability areas; (2) the species IUCN Redlist primate distribution polygons to quantify both the total number of species and the number of species we assessed for TDI occurring within each country's highest suitability areas; and (3) the dominant ecoregions<sup>41</sup> to identify habitat type associated with high suitable areas for sustained TIR drone surveys. Finally, we calculated the area (sq km) within each country to identify countries with the largest area of high TDI Suitability Scores and their correlation with the species contained therein (cf. steps 8 to 9 in the R script provided in Supplementary Material 3).

## Results

### Thermal detection indexes (TDIs)

We computed nocturnal and diurnal TDI for 389 primate species (database available in Supplementary Material 4). The average nocturnal TDI was  $8.1 \pm 1.4$  ( $TDI_{\min} = 5$  for 14 species sleeping in holes, tangles, cavities and caves such as *Aotus sp.*, *Leontocebus sp.*, *Papio sp.*, *Sciurocheirus sp.*, and *Trachypithecus sp.*;  $TDI_{\max} = 12$  for *Theropithecus gelada*). In contrast, the average diurnal TDI was lower with  $6.6 \pm 1.6$  ( $TDI_{\min} = 2$  for nine species with small body mass such as *Aotus sp.*, *Cheirogaleus sp.*, *Leontopithecus sp.*, *Microcebus sp.*, and *Sciurocheirus sp.*;  $TDI_{\max} = 11$  for *Theropithecus gelada*). There was a statistically significant difference between the nocturnal and diurnal TDI values (Welch's two-sample t-test;  $t = 12.78$ ,  $df = 758.06$ ,  $p\text{-value} < 0.001$ ) (Fig. 1). For both nocturnal and diurnal surveys, the families Atelidae, Cercopithecidae, and Indridae comprised species with the highest suitability for monitoring with a TIR drone, processing TDI values higher than the third quartile (nocturnal  $TDI > 9$  and diurnal  $TDI > 8$ ). Conversely, species within the families Aotidae, Callitrichidae, Cebidae, Cheirogaleidae, Daubentoniidae, Galagidae, Lepilemuridae, Lorisidae, Pithecidae were deemed less suitable for thermal drone surveys, processing TDI values lower than the first quartile (nocturnal  $TDI < 7$  and diurnal  $TDI < 6$ ) (Fig. 1). The differences between highest TDI ( $N_{\text{spp.}} = 58$ ) and lowest TDI ( $N_{\text{spp.}} = 25$ ) were predominantly driven by primate species body mass ( $BM_{\text{av.HIGH}} = 7.2 \pm 2.7$  kg and  $BM_{\text{av.LOW}} = 1.0 \pm 0.8$  kg), population densities ( $Dens_{\text{av.HIGH}} = 67.7 \pm 54.7$  sq km and  $Dens_{\text{av.LOW}} = 11.4 \pm 6.6$  sq km), and species detectability score during diurnal survey within different habitats (diurnal  $TDI_{\text{av.HIGH}} = 2.1 \pm 0.4$  and diurnal  $TDI_{\text{av.LOW}} = 1.4 \pm 0.9$ ).

### Global TDI suitability score

The regions exhibiting the highest cumulative TDI values within the global TDI layer were concentrated in central-west areas of Latin America, central-west regions in Africa, the east of Madagascar, Borneo, and the

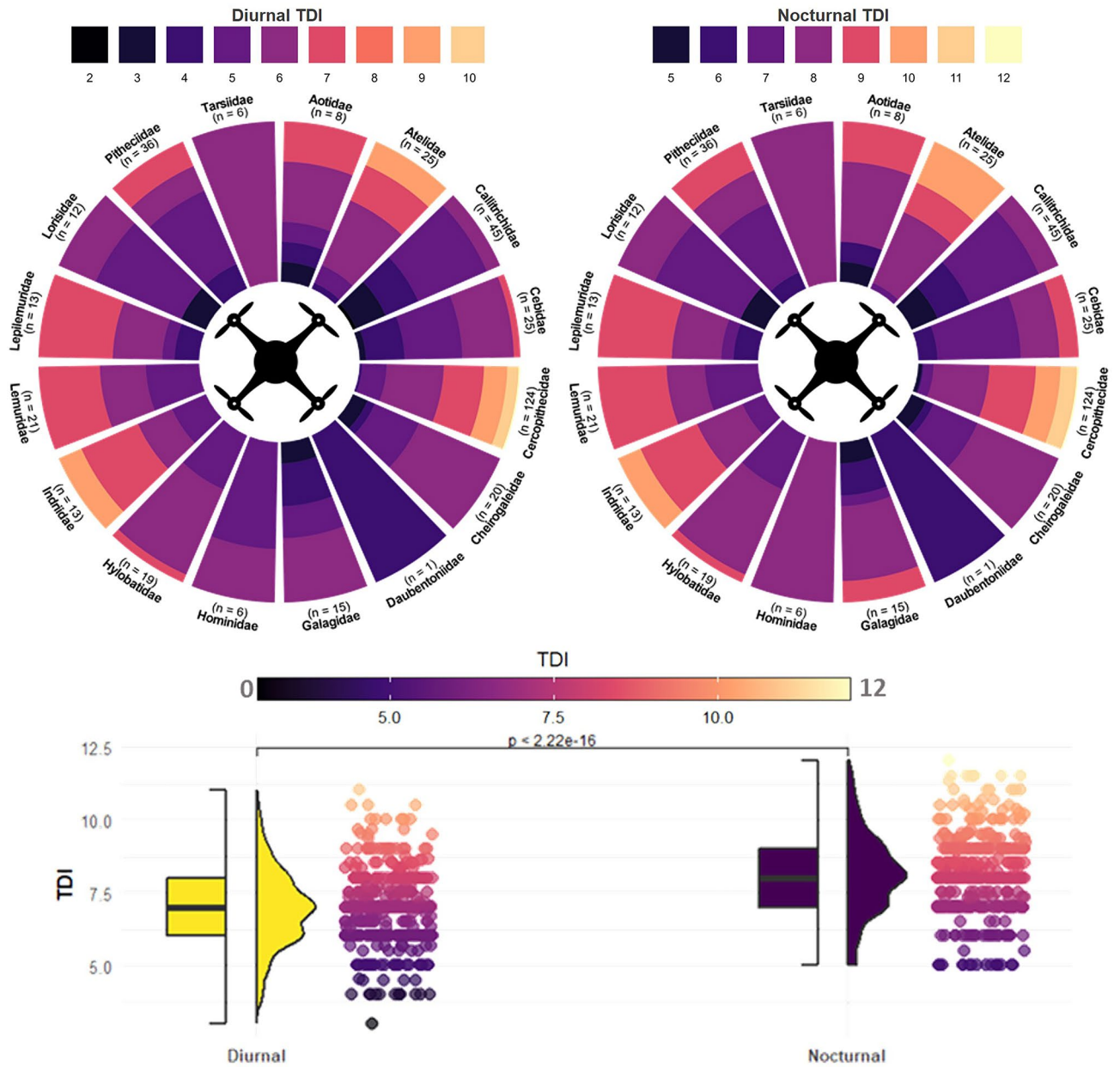


**Fig. 1.** Stacked bars depict the proportion (0–100%) of diurnal (left panel) and nocturnal (right panel) TDI values among primate species, grouped by family. Each stacked bar represents the percentage of species within the family assigned a specific TDI value rounded to the nearest integer. Lower TDI values indicate species less likely to be detected using thermal drone surveys, while higher TDI values suggest an elevated likelihood of detection. The lower panel features half box, violin, and jitter plots, highlighting a statistically significant difference in TDI values between diurnal and nocturnal survey methods.

eastern greater Mekong Sub-region (Fig. 2. b.). Subsequently, by applying normalization on the mean TDI values and normalized climatic data—specifically, average annual precipitation, annual average wind speeds, and annual average temperatures—to the global TDI layer (Fig. 2., c., d., e.), we generated a map illustrating the global TDI Suitability Score (Fig. 2. f.).

The highest suitability scores (0.75–1) were found in 34 countries (Table 3). Asia had the greatest proportion of suitable countries with highly suitable TDI areas relative to the total land area, averaging 20.53% ( $N=14$ ). This was followed by the Latin America, with an average of 5.89% per country ( $N=10$ ), and Africa, with an average of 4.94% per country ( $N=10$ ). Notably, 78% of Asian countries had moderate variability in TDI values, indicating more uniform species TDI values across the region, compared to 70% of African countries, which exhibited high variability, reflecting significant difference in species’ thermal detectability across the most suitable regions. Only India and Myanmar showed low TDI variability, suggesting minimal difference in species’ thermal detectability. In Africa, the highest species richness and the largest areas of high suitability were found

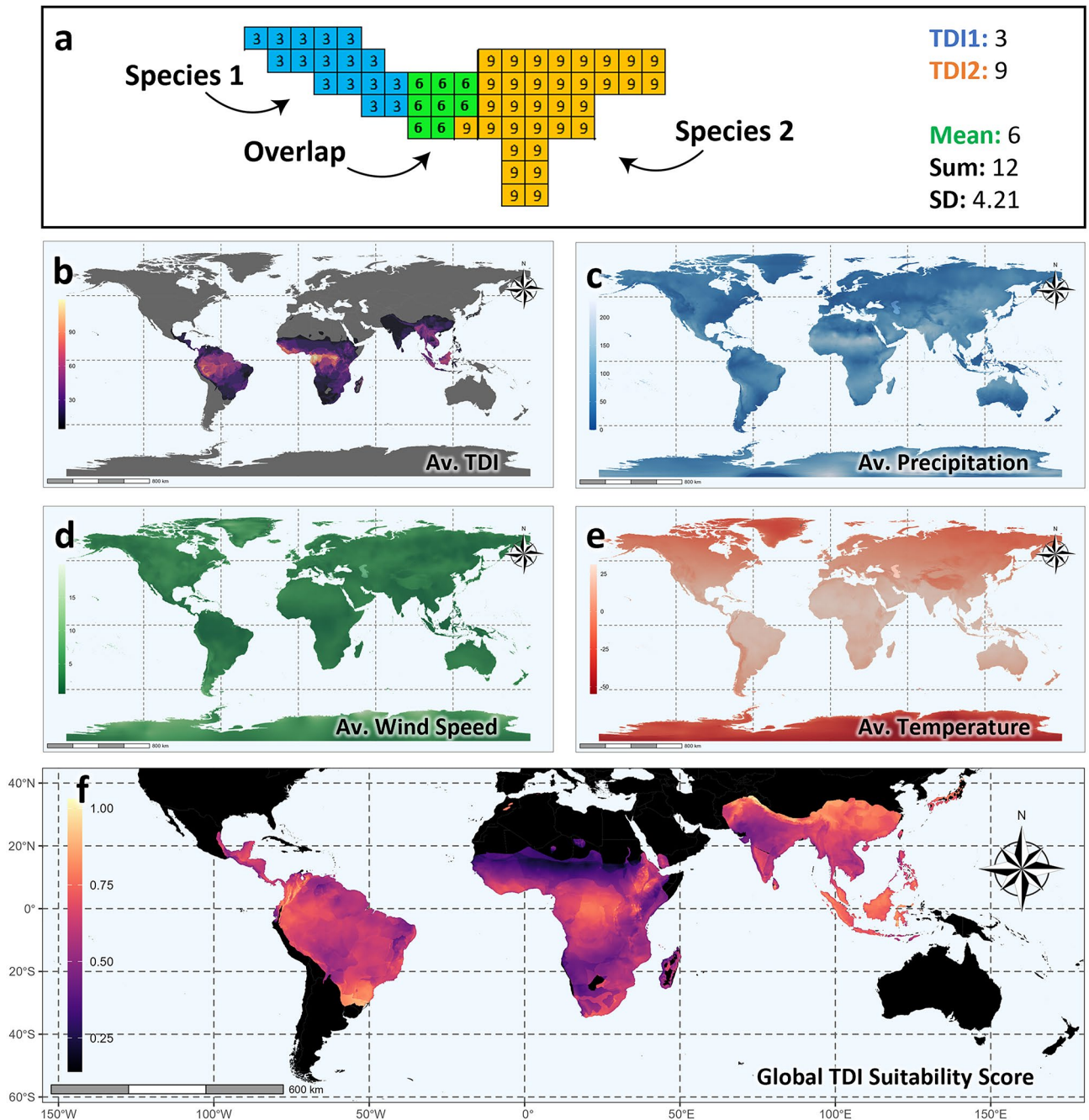


**Fig. 2.** The geospatial process of establishing a Thermal Detection Index (TDI) Suitability Score for primates across their global distributions: **a**) shows an example of rasterized distribution range shapefiles with associated TDI values as the cells, along with the cumulative, mean, and standard deviation values where they overlap. This process was used to generate **b**) the global cumulative TDI layer (average of Nocturnal and Diurnal TDI values), which was then used to calculate mean TDI values per grid cell and normalized to a 0–1 scale along with **c**) average annual precipitation, **d**) annual average wind speeds, and **e**) annual average temperatures. These climatic variables were processed as an inversely weighted relationship, where an increase of the three variables results in a decrease of the TDI value. The final outcome of this process is presented in **f**) the global TDI Suitability Score.

in the Democratic Republic of Congo, which had the largest landmass available (Table 3). In Asia, Indonesia had the highest number of species assessed for TDI within suitable areas ( $N_{\text{TDI spp.}} = 35$ ), while China had the largest area of high suitability (1,390,435.9 km<sup>2</sup>), covering 14.83% of its total land area. However, Buthan had the highest percentage of highly suitable area relative to its total land area (68.76%). In Latin America, Brazil had the highest number of overlapping species ( $N_{\text{tot spp.}} = 105$ ), covering 416,042.8 km<sup>2</sup> (4.91% of its total area), while Colombia had the largest relative suitable area (17.73%).

Country	$N_{\text{tot}}$ spp.	$N_{\text{TDI}}$ spp.	Suit. Area (km <sup>2</sup> )	Tot. Area (km <sup>2</sup> )	Relative Suit. Area	Variability
Africa						
Democratic Republic of the Congo	<b>32</b>	<b>28</b>	<b>402,097.0</b>	<b>2,324,449.6</b>	<b>17.30</b>	Moderate
Ethiopia	11	10	77,102.9	1,127,095.8	6.84	High
Kenya	17	10	22,129.5	592,189.9	3.74	High
Lesotho	2	2	2,968.6	29,991.1	9.9	High
Morocco	1	1	15,620.7	581,747.8	2.69	Moderate
Republic of Congo	26	18	432.3	345,334.0	0.13	High
Rwanda	16	14	1,696.7	25,272.6	6.71	High
South Africa	5	2	3,959.9	1,220,061.0	0.32	High
Tanzania	22	8	314.7	941,735.0	0.03	Moderate
Uganda	17	16	4,151.4	241,474.2	1.72	High
Asia						
Afghanistan	2	2	93,952.1	641,833.1	14.64	Moderate
Bhutan	6	6	27,375.0	39,811.3	<b>68.76</b>	Moderate
Brunei Darussalam	8	8	510.9	5,647.2	9.05	Moderate
China	23	15	<b>1,390,435.9</b>	<b>9,373,042.6</b>	14.83	Moderate
India	20	15	123,433.3	3,148,249.8	3.92	Low
Indonesia	<b>43</b>	<b>35</b>	567,841.4	1,863,914.9	30.46	Moderate
Japan	2	2	60,670.2	370,274.6	16.39	Moderate
Malaysia	20	19	201,078.9	326,202.4	61.64	Moderate
Myanmar	19	11	12,308.6	660,975.3	1.86	Low
Nepal	4	4	46,428.7	146,977.0	31.59	Moderate
Pakistan	2	2	107,911.1	872,783.0	12.36	Moderate
Philippines	3	2	19,601.3	289,182.4	6.78	Moderate
Sri Lanka	4	4	9,596.9	65,763.6	14.59	High
Thailand	17	6	2,877.5	513,909.8	0.56	Moderate
Latin America						
Argentina	6	6	141,258.5	2,782,471.6	5.08	High
Bolivia	28	2	3,322.5	1,086,628.6	0.31	Moderate
Brazil	<b>105</b>	<b>27</b>	<b>416,042.8</b>	<b>8,467,129.4</b>	4.91	High
Colombia	43	21	201,145.0	1,134,460.7	<b>17.73</b>	Moderate
Ecuador	18	14	37,468.0	254,528.7	14.72	High
Guatemala	4	2	303.9	108,101.8	0.28	Moderate
Paraguay	7	6	23,107.3	399,949.4	5.78	High
Peru	40	15	12,567.8	1,291,025.7	0.97	Moderate
Uruguay	1	1	10,420.7	177,467.5	5.87	Moderate
Venezuela	20	6	29,515.4	910,445.5	3.24	High

**Table 3.** Countries with highest Thermal Detection Index (TDI) suitability scores (0.75–1.0), the total number of species ( $N_{\text{tot}}$  spp.) overlapping in the country, and the number of species within the suitable area ( $N_{\text{TDI}}$  spp.), the total area of high suitability within each country, the country's total area, and the percentage of highly suitable area relative to the country's total area (%). Standard Deviation (variability) scores were categorized into low (<0.25), moderate (0.25–0.75), and high (>0.75). Bold numbers indicate the highest value for each category per continent.

The largest area of ecoregions by continent<sup>41</sup> within highly TDI Suitability areas were represented by central Congolian lowland forests (18.45%) and western and eastern Congolian swamp forests (7.15% combined) in Africa; Borneo lowland and montane rain forests (20.83% combined), Sumatran lowland and montane rain forests (7.27% combined), Southeast Tibet shrublands and meadows (3.29%), and Peninsular Malaysian rain forests (2.56%) in Asia; and Araucaria moist forests (2.51%) and Magdalena Valley montane forests (1.91%) in Latin America (Supplementary Material 5).

Countries with the highest TDI Suitability Scores had an average annual precipitation of  $1,589.6 \pm 805.4$  mm (range: 327.1–3,363.0 mm), average annual wind speeds of  $1.9 \pm 0.6$  m/s (range 0.9–3.4 m/s), and average annual temperatures of  $15.8 \pm 6.9$  °C (range: 3.2–25.2 °C) (Supplementary Material 6). African countries in the highest TDI suitability areas had the lowest average annual precipitation ( $1,217.1 \pm 503.0$  mm), wind speeds ( $1.8 \pm 0.6$  m/s), and temperatures ( $14.7 \pm 6.1$  °C). Asian countries showed medium average annual precipitation ( $1,739.6 \pm 978.0$  mm), wind speeds ( $1.9 \pm 0.6$  m/s), and temperatures ( $15.0 \pm 8.4$  °C). Latin American countries

presented the highest average annual precipitation ( $1,752.1 \pm 645.8$  mm), wind speeds ( $2.3 \pm 0.6$  m/s), and temperatures ( $18.1 \pm 4.4$  °C).

We found that 164 species occurred in the 34 highest TDI suitability areas, with 37 species in Africa, 57 in Latin America, and 70 in Asia. Specifically, species occurring in the largest landmasses with the highest TDI suitability scores included *Cercopithecus mitis* and *Colobus guereza* (family: Cercopithecidae) in Africa, *Alouatta seniculus* and *A. caraya* (family: Atelidae) in Latin America, and *Macaca assamensis* and *M. mulatta* (family: Cercopithecidae) in Asia. Latin American species in the highest TDI suitability areas exhibited relatively low average TDI values for arboreal species ( $\text{TDI}_{\text{Noc.}} = 7.5 \pm 1.9$ ;  $\text{TDI}_{\text{Diu.}} = 6.3 \pm 1.5$ ), largely due to smaller body mass (i.e.,  $\text{BM}_{\text{av.}} = 2.9$  kg, supplementary Table S5). In contrast, African species had medium average TDI values ( $\text{TDI}_{\text{Noc.}} = 8.2 \pm 1.6$ ;  $\text{TDI}_{\text{Diu.}} = 6.6 \pm 2.1$ ), mainly due to the presence of large-bodied species such as apes and baboons (e.g.,  $\text{BM}_{\text{av.}} = 14.7$  kg, supplementary Table S5). Finally, Asian species had relatively high average TDI values ( $\text{TDI}_{\text{Noc.}} = 8.8 \pm 1.2$ ;  $\text{TDI}_{\text{Diu.}} = 7.5 \pm 1.2$ ), primarily driven by higher detection scores across habitats during both nocturnal and diurnal surveys due to fewer species sleeping in holes or cavities and favorable habitat types for TIR detections (e.g., Artificial) (supplementary Table S5). Overall, primates species with the higher TDI values within suitable areas included *Alouatta arctoidea* and *A. caraya* (family: Atelidae) in Latin America, *Theropithecus gelada* (family: Cercopithecidae) in Africa, and *Semnopithecus vetulus* and *Trachypithecus germaini* (family: Cercopithecidae) in Asia (Supplementary Material 7).

## Discussion

Our study developed a Thermal Detection Index (TDI) to assess primate species and families with the highest suitability for monitoring with TIR drones based on species detectability during diurnal or nocturnal surveys and habitat types, as well as species-specific ecological, behavioral, and physiological traits. We identified that Atelidae, Cercopithecidae, and Indridae comprised species that were the most amenable to thermal drone monitoring, with species such as howler monkeys, geladas, and sifakas presenting the highest TDI values. These results are consistent with recent research that successfully used TIR drones to monitor forest-dwelling primates such as *Alouatta palliata*, *Ateles geoffroyi* and *Brachyteles arachnoides* from the Atelidae family in Latin America<sup>7,13,42</sup>, and *Macaca fascicularis*, *M. fuscata*, *M. leonina*, *Nasalis larvatus*, *Presbytis comata*, *Pygathrix cinerea*, *P. nigripes*, *Rhinopithecus roxellana*, *Trachypithecus auratus*, *T. delacouri*, *T. hatinhensis* and *T. margarita* from the Cercopithecidae family in Asia<sup>6,11,12,16,43,44</sup>. To the best of our knowledge, only *Propithecus tattersalli* from the Indridae family in Madagascar has been successfully monitored via RGB drone, but authors strongly recommend the use of thermal camera for further censuses on the species<sup>45</sup>. The highest nocturnal and diurnal TDIs were predominantly driven by high body mass, population densities, and detectability during diurnal surveys based on habitat characteristics, as well as locomotion type and sleeping habits. While the TDI construction inherently integrates these parameters, the observed patterns underscore the practical implications of our scoring system in identifying primate species most amenable to thermal detection. However, lower TDIs do not imply that certain families cannot be monitored, as the effectiveness of TIR drone surveys is species- and site-specific. For instance, studies have successfully used TIR drones to detect *Cebus imitator* from the Cebidae family in Latin America<sup>21</sup>; *Hylobates moloch*, *Nomascus gabriellae*, *N. hainanus* and *N. nasutus* from the Hylobatidae family<sup>6,8,9,16</sup>, and *Pongo pygmaeus* from the Hominidae family in Southeast Asia<sup>11</sup>. In a recent case study, we conducted manual and systematic nocturnal TIR drone surveys in southern Vietnam to assess the effectiveness of detecting and counting six diurnal, sympatric primate species at their sleeping sites<sup>12</sup>. Detection reliability was highest for large arboreal langurs (*P. nigripes*, *T. margarita*), followed by smaller-bodied, semi-arboreal macaques (*M. fascicularis*), and then semi-terrestrial macaques (*M. leonina*), with the lowest detection reliability observed for less abundant gibbons (*N. gabriellae*). The reliability of TIR drone detection at a short scale was influenced by primate physiological factors (e.g., body-size), ecological factors (e.g., group size and home range size), and sleeping site behavior (e.g., sleeping position in the canopy strata). These findings align with our TDI values, further validating the scoring system in assessing species most suitable for monitoring via thermal drones (Supplementary Material 4).

By integrating primate species distribution, TDIs, and bioclimatic variables (i.e., average annual temperature, wind speed, and annual precipitation), we propose a Global TDI Suitability Score that identifies suitable areas for more feasible and sustained TIR drone-based monitoring of primates. The northern and southern extents of South America, the Himalayas, Sundas region, Central Africa, and smaller hotspots in North Africa and Japan encompass areas with at least 75% suitability (Fig. 2, f, Table 3). Our results suggest that a combination of geographic, environmental, and physiological factors enables and optimizes both detection and TIR drone operability (Fig. 2, Supplementary Materials 5, 6, & 7). High TDI suitability scores in Brazil, China, Democratic Republic of the Congo, and Indonesia, may be driven by the large number of species, diverse habitats, and expansive suitable land areas in these regions. In Bhutan and Malaysia, where over 60% of the area is suitable for sustained TIR drone monitoring, environmental factors appear highly conducive to thermal detection (Table 3). Additionally, countries like Argentina and Ecuador, with high TDI variability, show fluctuating suitability, suggesting important environmental transitions for species adaptation. In contrast, India and Myanmar, with lower TDI variability, may have more stable thermal conditions that limit ecological niches<sup>46,47</sup>. Overall, in Latin America, the abundance of species in Araucaria and Montane forests<sup>41</sup> likely contributes to the highest TDI suitability scores. In contrast, the most suitable areas in Africa are characterized by dense lowland and swamp forests that support a high number of large-bodied species and favorable environmental conditions. Lastly, the highest suitability areas in Asia are influenced by ecosystems that support a substantial number of medium-bodied species sleeping in trees (Supplementary Materials 5, 6, & 7).

The occurrence of 164 primate species within the 34 highest TDI suitability areas highlights the significant biodiversity of these regions and their potential for effective TIR drone-based monitoring. The Atelidae and Cercopithecidae families contains species with the highest TDI values within the largest suitable areas, including



the highly arboreal *Alouatta* species in Latin America and *Cercopithecus*, *Macaca*, and *Trachypithecus* species, which exhibit a broader range of body sizes and ecological strategies across diverse environments in Africa and Asia. However, some countries or areas with low suitability scores for long-term TIR-drone monitoring could still be surveyed during more suitable climatic conditions in the short term (e.g., dry season in the tropics with low precipitation and cooler temperature)<sup>12</sup>. Finally, primate species with low TDI could still be good candidates for TIR drone monitoring if, for example, they are a single-ranging species in a relatively small study site.

Our new index and scoring system could assist further studies in identifying suitable primate species or countries for long-term monitoring with TIR drones. However, our results should be quantified depending on the context and goals of each study (e.g., long- or short-term monitoring). We recommend researcher to adapt the TDI and Global TDI suitability scores according to their study site and species-specific ecological traits (cf. R scripts in Supplementary Materials 2 & 3), as the metrics can be optimally localized based on existing knowledge of species body mass, local density, behavior, and habitat use. Furthermore, to improve the TDI, we could consider more specific ecological traits such as physical properties of the species' fur, as the thickness and/or color significantly affect the temperature of the outer surface of the body, such as darker fur absorbing more heat, and lighter fur reflecting it<sup>26</sup>. However, the low resolution of TIR drone imagery is a major limitation that makes it challenging to differentiate between species with similar morphology or behavior based solely on thermal imagery<sup>12,13,22</sup>. For study sites encompassing diverse mammal community with risks of misidentification, it is often recommended conducting a combination of TIR and RGB drone surveys or confirmed TIR detections via diurnal ground-truthing surveys<sup>16</sup>. In multispecies studies, we could consider adding a variable encompassing primate morphological traits 'complexity' that could help identification via TIR imagery (pending systematic methodologies) to the TDI scoring system. For example, large species with a long tail, and/or specific morphological traits such as prominent belly in douc langurs or proboscis monkeys would that be easier to detect than small species with no tail more likely to be misidentified with other small mammals<sup>12</sup>. Additionally, we recommend future studies to directly test the TDI metric by comparing species detection rates via TIR drones with densities obtained from traditional ground-based survey methods, such as line transects or censuses. Researchers could also conduct meta-analyses of primate studies in the intended survey area to gather localized information on primate species densities, group sizes, and ranges. Such comparison could help refine the index's accuracy at a localized scale and evaluate its consistency across different ecological contexts.

Similar improvements need to be considered for the Global TDI Suitability Score, as certain bioclimatic variables may not always be relevant depending on the study site or research objectives. For example, precipitations could serve as a positive factor by increasing the temperature difference between detected primate species and the surrounding vegetation. Additionally, while precipitation may limit the ability to fly drones, it can be minimal during certain seasons, allowing for short-term monitoring during dry periods in tropical countries. To develop a more accurate local TDI suitability scoring system, bioclimatic variables such as land-surface temperature, humidity, atmospheric pressure, and cloud cover could be considered, as these factors are known to strongly influence the absorption and emission of thermal infrared radiation by the atmosphere<sup>11,22,48</sup>. Furthermore, given the on-going rapid climate change, a global-scale assessment of primate vulnerability to climate change could be beneficial. For instance, Graham et al. (2016)<sup>39</sup> identified hotspots of primate vulnerability to global warming (i.e., significant temperature and/or precipitation changes). They found that species in Central America, the Amazon, southeastern Brazil, and portions of East and Southeast Asia, may face increased vulnerability. This assessment could effectively target regions requiring immediate research and conservation actions or those necessitating long-term monitoring.

Strict national laws and regulations governing the use of drones pose significant challenges to implement TIR drone monitoring. We did not consider the legal framework governing drone flights in each country when assessing the suitability of TIR drone surveys, given the frequently changing nature of these regulations<sup>49</sup>. Instead, we urge readers to investigate the legal regulations governing drone flight in their study sites, regardless of the suitability of TDI scoring for primate species or countries (e.g., consult community collated information in <https://www.droneregulations.info/> and <https://drone-laws.com/><sup>50</sup>) and to read the drone regulations for each specific country which is often available through the civil aviation authority website. Additionally, nocturnal surveys are generally more favorable for primate species detections, but some countries do not allow night surveys<sup>49,51,52</sup>. Therefore, we recommend favoring a combination of TIR and RGB drone surveys during the day to assist species identification in sub-optimal conditions for TIR imagery detection<sup>12,16,21</sup>. Moreover, many countries' regulations stipulate that flights should be conducted within visual or extended line of sight (i.e., 500–750 m), which is often not feasible in dense tropical forest due to trees limiting visual line of sight and hence reduce the distance a drone can be flown<sup>5,12</sup>.

To conclude, our study provides comprehensive results and tools for improving research to identify optimal candidates for TIR drone monitoring in primatology. We synthesized our results, including average Thermal Detection Index (TDI) and Global TDI Suitability Score, for 389 primate species across their global distributions on the HTML flexdashboard and map Online ([https://rpubs.com/Russell\\_Gray/GlobalPrimateTDI](https://rpubs.com/Russell_Gray/GlobalPrimateTDI)). Our findings have significant implications for both research and conservation efforts in the following ways: (1) Enhanced primate monitoring: our results facilitate targeted monitoring programs by prioritizing species based on detectability and habitat suitability, thereby improving resource allocation and monitoring efficiency. (2) Informed conservation strategies: identification of areas with high TDI suitability scores enables the planning and implementation of targeted conservation surveys, maximizing the impact on threatened primate populations. (3) Global monitoring initiatives: our study contributes to global efforts in systematic TIR drone surveys by providing tools to assess primate detectability. (4) Technological advancements: integration of TDI-based approaches expands the range of tools available for wildlife research and conservation, enhancing data collection accuracy and informing management decisions. Our study represents a critical step towards advancing primate monitoring and conservation efforts through the integration of TIR drone surveys.

## Data availability

The datasets generated and analysed during this study are included in this published article and its Supplementary Information files. All Supplementary Materials and data can be found in our OSF server (<https://osf.io/j4hfw>).

Received: 5 June 2024; Accepted: 23 October 2024

Published online: 14 November 2024

## References

- Christie, K. S., Gilbert, S. L., Brown, C. L., Hatfield, M. & Hanson, L. Unmanned aircraft systems in wildlife research: current and future applications of a transformative technology. *Front. Ecol. Environ.* **14** (5), 241–251. <https://doi.org/10.1002/fee.1281> (2016).
- Howell, L. G. et al. Drone thermal imaging technology provides a cost-effective tool for landscape-scale monitoring of a cryptic forest-dwelling species across all population densities. *Wildl. Res.* **49** (1), 66–78. <https://doi.org/10.1071/WR21034> (2021).
- Jiménez López, J. & Mulero-Pázmány, M. Drones for conservation in protected areas: present and future. *Drones*. **3** (1), 10. <https://doi.org/10.3390/drones3010010> (2019).
- Wich, S. A., Hudson, M., Andrianandrasana, H. & Longmore, S. N. Drones for conservation in Conservation Technology (eds Wich, S. A. & Piel, A. K.) 35–51. Oxford University Press; <https://doi.org/10.1093/oso/9780198850243.003.0003> (2021).
- Wich, S. A. & Koh, L. P. *Conservation Drones: Mapping and Monitoring Biodiversity* (Oxford University Press, 2018). <https://doi.org/10.1093/oso/9780198787617.001.0001>
- Gazagne, E., Gray, R. J., Ratajszczak, R., Brotcorne, F. & Hamburgers, A. Unmanned aerial vehicles (UAVs) with thermal infrared (TIR) sensors are effective for monitoring and counting threatened Vietnamese primates. *Primates*. 1–7. <https://doi.org/10.1007/s10329-023-01066-9> (2023).
- Spaan, D. et al. A. Thermal infrared imaging from drones offers a major advance for spider monkey surveys. *Drones*. **3** (2), 34. <https://doi.org/10.3390/drones3020034> (2019).
- Wearn, O. R., Trinh-Dinh, H., Le, Q. K. & Nguyen, T. D. UAV-assisted counts of group size facilitate accurate population surveys of the critically endangered cao vit gibbon *Nomascus Nasutus*. *Oryx*. 1–4 <https://doi.org/10.1017/S0030605323000017> (2023).
- Zhang, H. et al. Commercial drones can provide accurate and effective monitoring of the world's rarest primate. *Remote Sens. Ecol. Conserv.* **9** (6), 775–786. <https://doi.org/10.1002/rse2.341> (2023).
- Brack, I. V., Kindel, A. & Oliveira, L. F. B. Detection errors in wildlife abundance estimates from unmanned Aerial systems (UAS) surveys: synthesis, solutions, and challenges. *Methods Ecol. Evol.* **9** (8), 1864–1873. <https://doi.org/10.1111/2041-210X.13026> (2018).
- Burke, C. et al. Successful observation of orangutans in the wild with thermal-equipped drones. *J. Unmanned Veh. Syst.* **7** (3), 235–257. <https://doi.org/10.1139/juvs-2018-0035> (2019).
- Gazagne, E., Gray, R. J., Nguyễn, V. T. & Brotcorne, F. Effectiveness of thermal infrared drone surveys in detecting the diurnal primate community in Cat Tien National Park, South Vietnam. *Viet J. Primatol.* **3**(5) (2024).
- Kays, R. et al. Hot monkey, cold reality: surveying rainforest canopy mammals using drone-mounted thermal infrared sensors. *Int. J. Remote Sens.* **40** (2), 407–419. <https://doi.org/10.1080/01431161.2018.1523580> (2019).
- Pagacz, S. & Witczuk, J. Estimating ground surface visibility on thermal images from drone wildlife surveys in forests. *Ecol. Inf.* **78**, 102379 (2023).
- Brunton, E. A., Leon, J. X. & Burnett, S. E. Evaluating the efficacy and optimal deployment of thermal infrared and true-colour imaging when using drones for monitoring kangaroos. *Drones*. **4** (2), 20. <https://doi.org/10.3390/drones4020020> (2020).
- Rahman, D. A., Sitorus, A. B. Y. & Condoro, A. A. From coastal to montane forest ecosystems, using drones for multi-species research in the tropics. *Drones*. **6** (1), 6. <https://doi.org/10.3390/drones6010006> (2022).
- Greene, K., Bell, D., Kioko, J. & Kiffner, C. Performance of ground-based and aerial survey methods for monitoring wildlife assemblages in a conservation area of northern Tanzania. *Eur. J. Wildl. Res.* **63**, 1–13. <https://doi.org/10.1007/s10344-017-1133-2> (2017).
- Linchant, J., Lisein, J., Semeki, J., Lejeune, P. & Vermeulen, C. Are unmanned aircraft systems (UASs) the future of wildlife monitoring? A review of accomplishments and challenges. *Mamm. Rev.* **45** (4), 239–252. <https://doi.org/10.1111/mam.12046> (2015).
- Hambrech, L., Brown, R. P., Piel, A. K. & Wich, S. A. Detecting 'poachers' with drones: factors influencing the probability of detection with TIR and RGB imaging in miombo woodlands, Tanzania. *Biol. Conserv.* **233**, 109–117. <https://doi.org/10.1016/j.BIOCON.2019.02.017> (2019).
- Rahman, D. A. & Setiawan, Y. Possibility of applying unmanned aerial vehicle and thermal imaging in several canopy cover class for wildlife monitoring—preliminary results. In E3S Web of Conferences (Vol. 211, p. 04007). EDP Sciences; <https://doi.org/10.1051/e3sconf/202021104007> (2020).
- Whitworth, A., Pinto, C., Ortiz, J., Flatt, E. & Silman, M. Flight speed and time of day heavily influence rainforest canopy wildlife counts from drone-mounted thermal camera surveys. *Biodivers. Conserv.* **31** (13–14), 3179–3195. <https://doi.org/10.1007/s10531-022-02483-w> (2022).
- Burke, C. et al. Optimizing observing strategies for monitoring animals using drone-mounted thermal infrared cameras. *Int. J. Remote Sens.* **40** (2), 439–467. <https://doi.org/10.1080/01431161.2018.1558372> (2018).
- Duporge, I. et al. Determination of optimal flight altitude to minimise acoustic drone disturbance to wildlife using species audiograms. *Methods Ecol. Evol.* **12** (11), 2196–2207. <https://doi.org/10.1111/2041-210X.13691> (2021).
- Schad, L. & Fischer, J. Opportunities and risks in the use of drones for studying animal behaviour. *Methods Ecol. Evol.* **14** (8), 1864–1872. <https://doi.org/10.1111/2041-210X.13922> (2022).
- Karp, D. Detecting small and cryptic animals by combining thermography and a wildlife detection dog. *Sci. Rep.* **10** (1), 5220. <https://doi.org/10.1038/s41598-020-61594-y> (2020).
- Ciulko, J., Janiszewski, P., Bogdaszewski, M. & Szczygielska, E. Infrared thermal imaging in studies of wild animals. *Eur. J. Wildl. Res.* **59**, 17–23. <https://doi.org/10.1007/s10344-012-0688-1> (2013).
- Gao, M. et al. Weather constraints on global drone flyability. *Sci. Rep.* **11** (1), 12092. <https://doi.org/10.1038/s41598-021-91325-w> (2021).
- Havens, K. J. & Sharp, E. J. Thermal imaging techniques to survey and monitor animals in the wild: a methodology. Academic Press, Elsevier; (2016). <https://doi.org/10.1016/C2014-0-03312-6>
- Zabel, F., Findlay, M. A. & White, P. J. Assessment of the accuracy of counting large ungulate species (red deer *Cervus elaphus*) with UAV-mounted thermal infrared cameras during night flights. *Wildl. Biol.* e01071. <https://doi.org/10.1002/wlb3.01071> (2023).
- IUCN Redlist. The IUCN Red list of threatened species. Version 2023-1. <https://www.iucnredlist.org>. (2024). Accessed on 9 Feb 2024.
- Galán-Acedo, C., Arroyo-Rodríguez, V., Andresen, E. & Arasa-Gisbert, R. Ecological traits of the world's primates database. *Zenodo*. <https://doi.org/10.5281/zenodo.2600338> (2019).
- Pozzi, L., Voskamp, M. & Kappeler, P. M. The effects of body size, activity, and phylogeny on primate sleeping ecology. *AJBA*. **179** (4), 598–608. <https://doi.org/10.1002/ajpa.24640> (2022).

33. Fick, S. E., Hijmans, R. J., WorldClim 2. New 1-km spatial resolution climate surfaces for global land areas. *Int. J. Climatol.* **37**(12), 4302–4315. <https://doi.org/10.1002/joc.5086> (2017).
34. Granatosky, M. C. A review of locomotor diversity in mammals with analyses exploring the influence of substrate use, body mass and intermembral index in primates. *J. Zool.* **306** (4), 207–216. <https://doi.org/10.1111/jzo.12608> (2018).
35. Witczuk, J., Pagacz, S., Zmarz, A. & Cypel, M. Exploring the feasibility of unmanned aerial vehicles and thermal imaging for ungulate surveys in forests—preliminary results. *Int. J. Remote Sens.* **39** (15–16), 5504–5521. <https://doi.org/10.1080/01431161.2017.1390621> (2018).
36. Mutalib, A. H. A., Ruppert, N., Kamaruzaman, S. A., Jamsari, F. F. & Rosely, N. F. N. Feasibility of thermal imaging using unmanned aerial vehicles to detect bornean orangutans. *J. Sustain. Sci. Manag.* **14** (5), 182–194 (2019).
37. Pebesma, E. & Bivand, R. *Spatial Data Science: With Applications in R (1st ed.)*. 314 pages (Chapman and Hall/CRC, Boca Raton, 2023). <https://doi.org/10.1201/9780429459016>.
38. Hijmans, R. J. raster. *Geographic Data Analysis and Modeling. R package version 3.6–26* (2023) <https://CRAN.R-project.org/package=raster>.
39. Graham, T. L., Matthews, H. D. & Turner, S. E. A global-scale evaluation of primate exposure and vulnerability to climate change. *Int. J. Primatol.* **37**, 158–174. <https://doi.org/10.1007/s10764-016-9890-4> (2016).
40. Zurell, D. & Engler, J. O. Ecological niche modeling in *Effects of Climate Change on Birds* Second Edition (Eds. Dunn, P. O., & Moller, A. P.) 60–73. Oxford University Press. <https://doi.org/10.1093/oso/9780198824268.003.0006>. (2019).
41. Dinerstein, E. et al. An ecoregion-based approach to protecting half the terrestrial realm. *Biosci.* **67** (6), 534–545. <https://doi.org/10.1093/biosci/bix014> (2017).
42. de Melo, F. R. Drones for conservation: new techniques to monitor muriquis. *Oryx.* **55** (2), 171–171. <https://doi.org/10.1017/S003065321000028> (2021).
43. He, G. et al. Undertaking wildlife surveys with unmanned aerial vehicles in rugged mountains with dense vegetation: a tentative model using Sichuan Snub-nosed monkeys in China. *GECCO.* **48**, 85. <https://doi.org/10.1016/j.gecco.2023.e02685> (2023).
44. Mirka, B. et al. Evaluation of thermal infrared imaging from uninhabited aerial vehicles for arboreal wildlife surveillance. *Environ. Monit. Assess.* **194** (7), 512. <https://doi.org/10.1007/s10661-022-10152-2> (2022).
45. Semel, B. P., Karpanty, S. M., Vololonirina, F. F. & Rakotonanahary, A. N. Eyes in the sky: assessing the feasibility of low-cost, ready-to-use unmanned aerial vehicles to monitor primate populations directly. *Folia Primatol.* **91** (1), 69–82. <https://doi.org/10.1159/00496971> (2019).
46. Eppley, T. M., Hoeks, S., Chapman, C. A., Ganzhorn, J. U., Hall, K., Owen, M. A., ... Santini, L. Factors influencing terrestriality in primates of the Americas and Madagascar. *PNAS* **119**(42), e2121105119; <https://doi.org/10.1073/pnas.2121105119> (2022).
47. Macho, G. A. From rainforests to savannas and back: the impact of abiotic factors on non-human primate and hominin life histories. *Quat Int.* **448**, 5–13. <https://doi.org/10.1016/j.quaint.2016.04.022> (2017).
48. Hill, R. A., Weingrill, T., Barrett, L. & Henzi, S. P. Indices of environmental temperatures for primates in open habitats. *Primates.* **45**, 7–13. <https://doi.org/10.1007/s10329-003-0054-8> (2004).
49. Ravich, T. A. & Comparative Global Analysis of Drone Laws: best Practices and Policies in *The Future of Drone Use, Opportunities and Threats from Ethical and Legal Perspectives* (ed. Custers, B.) 301–322. (T. M. C. Asser P, (2016). [https://doi.org/10.1007/978-94-6265-132-6\\_16](https://doi.org/10.1007/978-94-6265-132-6_16) (2016).
50. Duffy, J. P. et al. Location, location, location: considerations when using lightweight drones in challenging environments. *Remote Sens. Ecol. Conserv.* **4** (1), 7–19. <https://doi.org/10.1002/rse2.58> (2017).
51. Cracknell, A. P. UAVs: regulations and law enforcement. *Int. J. Remote Sens.* **38** (8–10), 3054–3067. <https://doi.org/10.1080/01431161.2017.1302115> (2017).
52. Tran, T. H. & Nguyen, D. D. Management and regulation of drone operation in urban environment: a case study. *Soc. Sci.* **11** (10), 474. <https://doi.org/10.3390/socsci11100474> (2022).

## Acknowledgements

This research was conducted with the financial support of the Belgian National Fund for Scientific Research (FNRS) and the University of Liège. We would like to thank the two anonymous reviewers for their valuable feedback and constructive suggestions, which greatly contributed to improving this manuscript.

## Authors' contributions

E.G. and R.J.G. conceptualized the research. E.G. wrote the main manuscript text and prepared tables. R.J.G. prepared figures. E.G. and R.J.G. developed Online Resource S1. R.J.G. wrote Online Resource S2. E.G. and R.J.G. conducted statistical analyses. S.W., A.H., and F.B. reviewed the manuscript. All authors agreed to the published version of the manuscript.

## Declarations

### Competing interests

The authors declare no competing interests.

## Additional information

**Supplementary Information** The online version contains supplementary material available at <https://doi.org/10.1038/s41598-024-77502-7>.

**Correspondence** and requests for materials should be addressed to E.G.

**Reprints and permissions information** is available at [www.nature.com/reprints](http://www.nature.com/reprints).

**Publisher's note** Springer Nature remains neutral with regard to jurisdictional claims in published maps and institutional affiliations.

**Open Access** This article is licensed under a Creative Commons Attribution-NonCommercial-NoDerivatives 4.0 International License, which permits any non-commercial use, sharing, distribution and reproduction in any medium or format, as long as you give appropriate credit to the original author(s) and the source, provide a link to the Creative Commons licence, and indicate if you modified the licensed material. You do not have permission under this licence to share adapted material derived from this article or parts of it. The images or other third party material in this article are included in the article's Creative Commons licence, unless indicated otherwise in a credit line to the material. If material is not included in the article's Creative Commons licence and your intended use is not permitted by statutory regulation or exceeds the permitted use, you will need to obtain permission directly from the copyright holder. To view a copy of this licence, visit <http://creativecommons.org/licenses/by-nc-nd/4.0/>.

© The Author(s) 2024